CORROSION SCIENCE AND TECHNOLOGY, Vol.2, No.3(2003), pp.135~140

The Effect of Temperature on Stress Corrosion Cracking of Al Brass under Flow

Uh Joh Lim and Hae Kyoo Jeong*

Department of mechanical Engineering, Pukyong National University
San 100 YongDangDong, NamGu, Pusan, 607-739, KOREA
Outffiting Design Department No.3, Hyundai Heavy Industry Company
JeonHaDong, DongGu, Ulsan, KOREA

The effect of temperature on stress corrosion cracking of Al-brass used in vessel heat exchanger tube was studied in 3.5% NaCl + 0.1% NH_4OH solution. The SCC test using a CDT(constant displacement test) and the specimens using a SEN(single edge notched) specimens. For setting the environment similar to working environment of a heat exchanger, the specimens was immersed in solution and solution flow onto the specimens were performed. The results are as follows : The latent time of stress corrosion crack occurrence gets shorter, as the temperature gets higher. Dezincification phase showed around the crack occupy wider range, as the temperature gets higher. Zn composition falls under 4% at the dezincifiction area.

Keywords *: single edge notched specimen, constant displacement test, dezincification.*

1. Introduction

Shell and tube type heat exchangers are operated with several heat medium such as sea water, tap water, lubricant, fuel, steam under wide range of temperature and flow rate. They also have to endure vibration of vessel. Seal methods of tube's expansion, pertain residual stress by deformation. Fishes and shells cause higher local flow rate on those inlet area of seawater. It is reported that those situation makes local corrosion damage of Al-brass such as erosion, pitting and stress corrosion cracking.

Al-brass is the raw material of manufacturing tubes for heat exchanger where seawater is used as a cooling water because it has high level of heat conductivity and excellent mechanical properties and high level of corrosion resistance due to cuprous oxide (Cu_2O) layer against seawater.

In general, entrance temperature of cooling sea water for oil cooler is about 25 ℃ and exit temperature is about 40 ℃. For steam turbine condenser, entrance temperature of cooling sea water is around 25 ℃ and exit temperature is around 60 ℃, but since the temperature of the coolant heavily depends on the design of a heat exchanger system. It is necessary to set the temperature of the cooling water to have maximum heat transfer efficiency.

In this paper, the effect of temperature on SCC of Al-brass, the SCC test using a CDT(constant displacement test) and the specimens using a SEN(single edge notched) specimens. For setting the environment similar to working environment of a heat exchanger, the specimens was immersed in 3.5% NaCl + 0.1% NH_4OH solution and solution flow onto the specimens were performed. Based on the test results, the behavior of stress corrosion crack propagation of Al-brass was examined. The correlation between dezincification and temperature of solution was investigated.

2. Experimental apparatus and method

The material of test specimen in this study is Al-brass, generally used for shell and tube type heat exchanger. Table 1. shows the chemical compositions and mechanical properties of Al-brass. The property of specimen cut from Al-brass tube(C6870T) showed in Table 1. It is processed with low speed to minimize heat effect and then, abrased by sand paper(#800-1200) and washed with aceton.

Table 1. Chemical compositions and mechanical properties of Al-brass(C6870T)

Chemical composition (wt %)	Cu	Pb	Fe	Al	As	Zn
	76.0	0.05	0.05	1.85	0.02	Remainder
Mechanical properties	Tensile Strength (MPa)		Yield Strength (MPa)	Hardness (HR30T)	Elongation (%)	Grain Size (μm)
	345		125	-	39	40

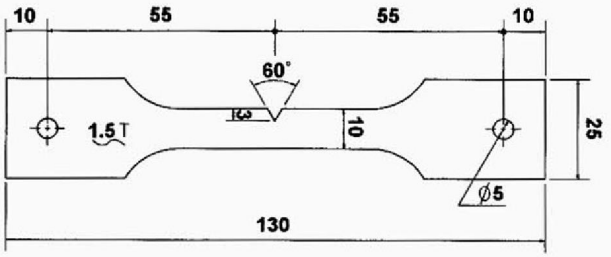

Fig. 1. Dimension of single edge notched test specimen(unit : mm)

Fig. 1 shows shape and dimension of the specimen which made into SEN[1](Single Edge Notched). Notch radius of the specimen is 0.2 mm and initial stress intensity factor KIi at notch edge was calculated with Equation (1).[2]

$$K_{Ii} = Y\sigma \sqrt{a} \quad (1)$$

$$Y = 1.99 - 0.41\lambda + 18.70\lambda^2 - 38.48\lambda^3 + 53.85\lambda^4$$

λ = a/w, a=length of notch, w=width of specimen

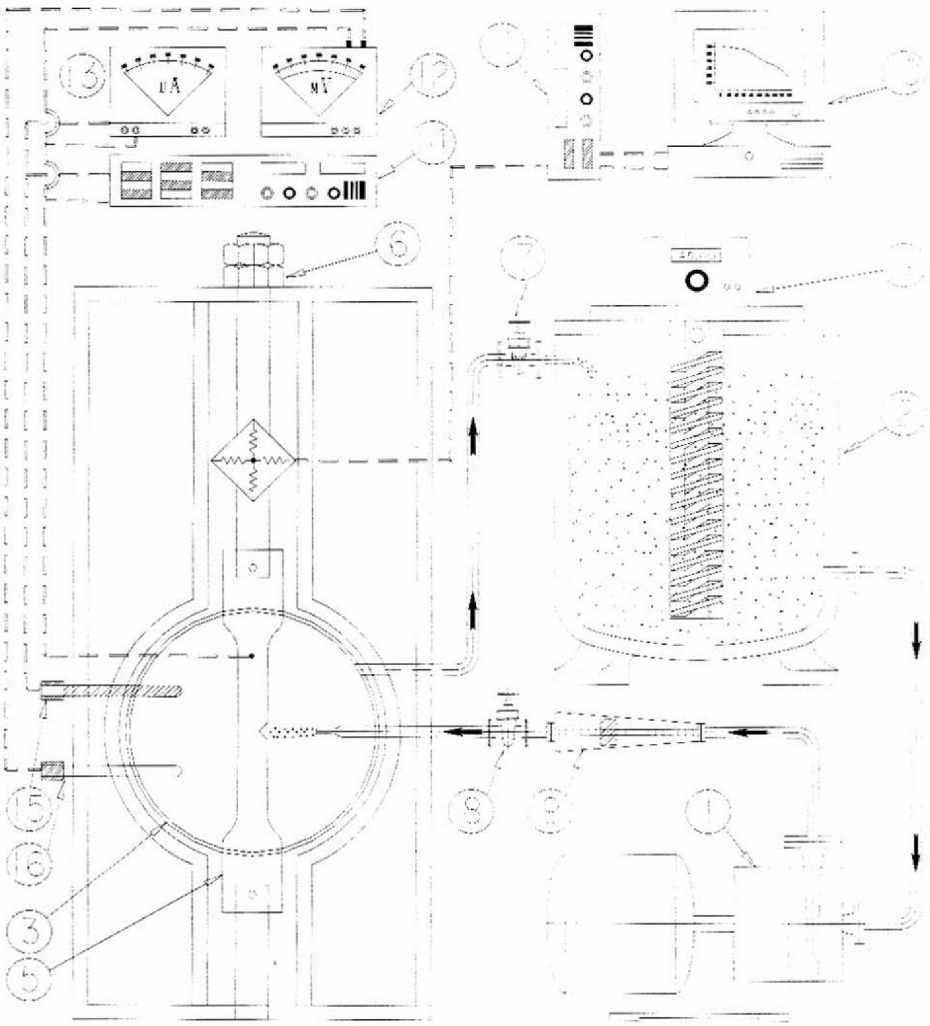

1. Magnetic pump
2. Test liquid tank
3. Test liquid chamber
4. Cylinder type heater
5. Specimen
6. Tension jig with load cell
7. Supply control valve
8. Discharge control valve
9. Flowmeter
10. Computer
11. A/D convert
12. Potentiometer
13. Ampere meter
14. Power supply
15. Counter electrode
16. Reference electrode

Fig. 2. Schematic diagram of stress corrosion cracking test apparatus

Fig. 2 shows schematic diagram of stress corrosion cracking under flow test apparatus used in this study. The tensile tester in Fig. 2 is the constant displacement tester. It is designed that we can control the applied loads by tension jig and bolt after the specimen attached into tensile tester. Applied load data were recorded by using computer database through load cell and AD convert connected with the specimen. And solution flow part in Fig. 2 is manufactured through magnetic pump and glass cylinder type heater to minimize effect of electro-chemical corrosion through experiments. Pipes, solution tank and valves made by plastic were used. To study behavior of stress corrosion cracking of the specimen under flow, the nozzle(ϕ 5 mm) was attached at the 50 mm top of the specimen. Solution velocity was controlled within 0 m/s ~ 9 m/s by valve and flowmeter. To control solution temperatures, heater was equipped at water tank and heat controller was used to control temperature from room temperature up to 75℃. To prevent leakage, each joint segment was wrapped with rubber ring.

To study the effect of solution temperature on stress corrosion cracking of Al-brass under flow, initial applied stress(σ) was applied with 75 %(94 MPa) of yield stress(σ_y). Using Equation (1), initial stress intensity factor(K_{Ii}) was calculated with 657 $N \cdot mm^{-3/2}$. To accelerate the test period, 0.1% NH_4OH were added in 3.5% NaCl solution. The temperatures of the solution were changed at 25℃, 30℃ 45℃ and 60℃ ±1℃. The specimens were immersed in solution and the solution was injected onto surface of specimens with the velocity of 5 m/s. It took 160 hours total to do experiment. To measure the crack length, magnifier was used after stopping circulation of the solution. Dial gauge was set in the direction of applied load at the tester to compare with the real cracking propagation rate. After the test, the specimen was detached, abrased, washed in supersonic washer with alcohol, for removed fat, dried, soaked into 25g $FeCl_3$ + 25 ml HCl + 100ml solution for 20 seconds for etching[3] and then, examined with SEM equipped with EDS(Energy Dispersive Spectrometer).

3. Results and discussion

3.1 Stress corrosion cracking propagation behavior

Fig. 3 shows stress corrosion crack propagation behavior of Al-brass according to the change of temperature in 3.5% NaCl + 0.1% NH_4OH solution injected onto the specimen under initial stress with 75 % of yield stress. It shows that the higher temperature of the solution, the faster the stress corrosion crack propagation rate of Al-brass. The above result can be considered as follows. While going up the temperature, stress- mechanical factor

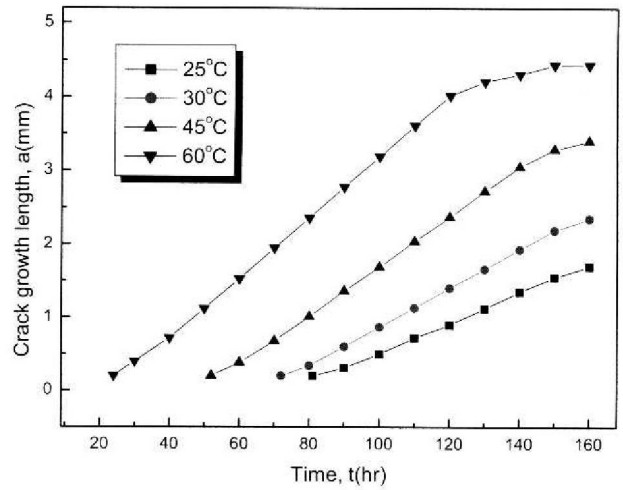

Fig. 3. Crack growth length vs test time(hr) in 3.5% NaCl + 0.1% NH_4OH solution(v = 5 m/s) at 75%σ_y(94 MPa)

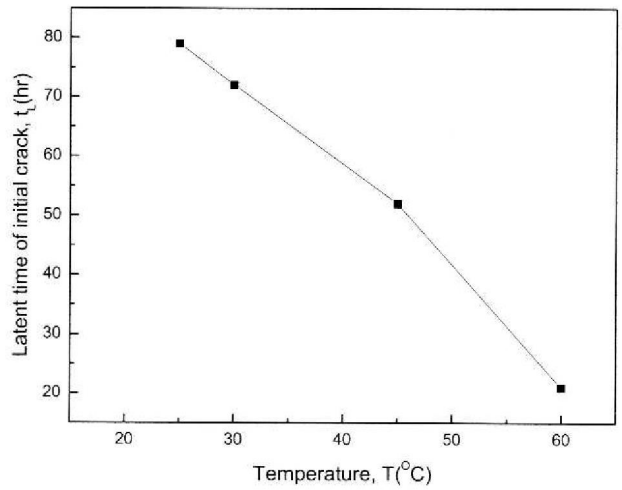

Fig. 4. Latent time of initial crack vs temperature of 3.5% NaCl + 0.1% NH_4OH solution(v = 5 m/s) at 75%σy(94 MPa)

remains the same, but the molecular activity of oxygen and ammonia-electrochemical factor cause active corrosion such as a fast dezincification.[4),5)] And cracking propagation was stopped after the crack size increased to 4.5 mm at 60℃ solution. The reason is that the experimental instrument of this study is the constant displacement tester.

Fig. 4 shows the relation between solution temperature and latent time(standard crack length : 0.2 mm) of crack occurrence after beginning stress corrosion test. It shows that as the temperature of the solution gets higher, the occurrence time of initial crack from notch edge becomes shorter rapidly.

As shown in Fig. 3 and Fig. 4, the crack propagation rate gets higher and latent period gets rapidly shorter as

the temperature of the solution increases even though initial load stress remains same. It is concluded that galvanic circuit formed bigger between slip trace area by tensile stress and other area in ammonia solution.[6),7)]

3.2 Stress corrosion cracking damage phase

Photo. 1(a) shows stress corrosion crack fractography in 30 ℃ solution. It shows that crack grows following slip step of slip trace at the maximum shear stress of notch. Photo. 1(b) is a magnified picture crack face of A in the Photo. 1(a). Around the crack, there are pits formed which is similar with micro-crack. And it is concluded that dezincification phase also was found around the pit and the micro-crack.

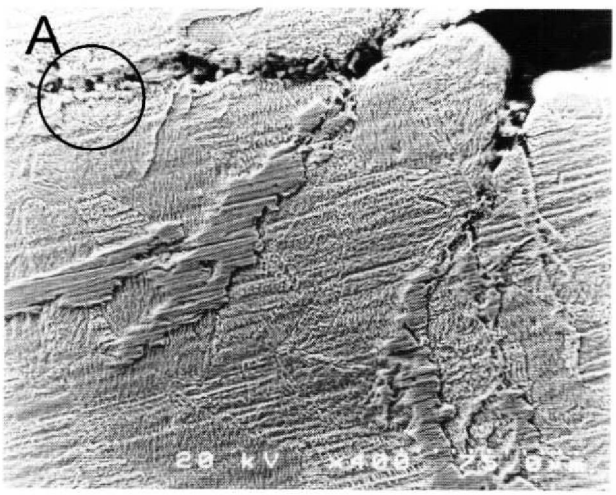

(a) Crack propagation

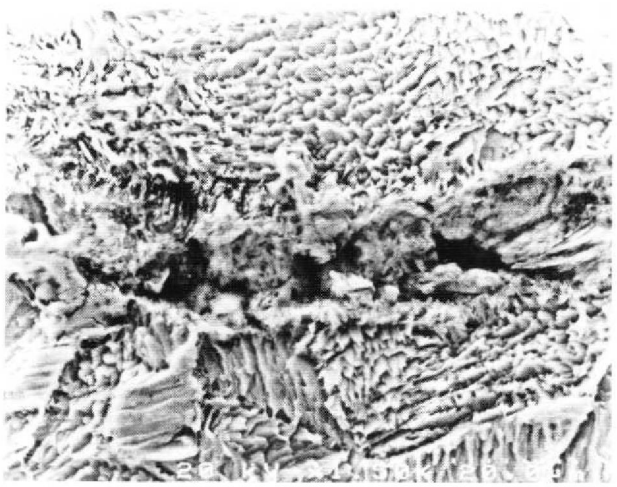

(b) Crack tip of A region

Photo. 1. SEM fractography of SCC in 30℃, 3.5% NaCl + 0.1% NH_4OH solution(v = 5 m/s) at 75%σy(94 MPa)

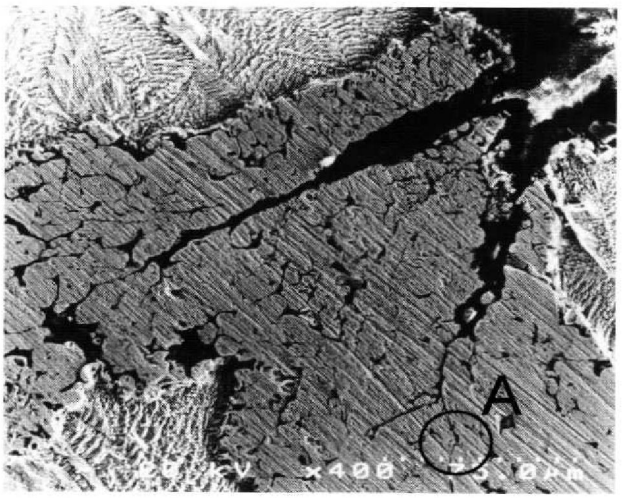

(a) Crack propagation

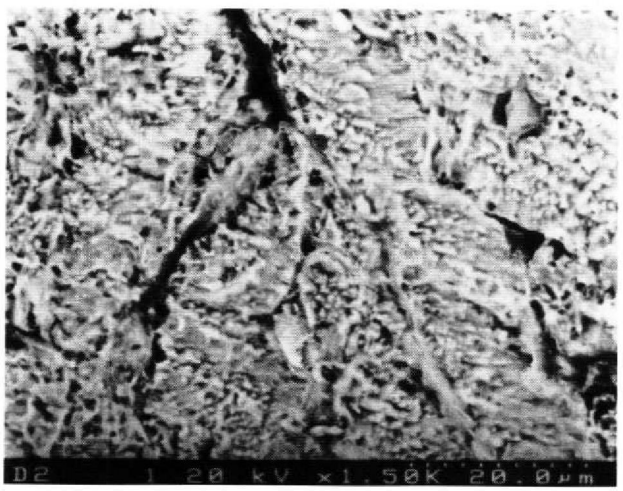

(b) Crack tip of (A) region

Photo. 2. SEM fractography observed in 45℃, 3.5% NaCl + 0.1% NH_4OH solution(v = 5 m/s) at 75%σy(94 MPa)

Photo. 2(a) shows stress corrosion crack fractography in 45 ℃ solution. It shows that crack grows following slip step of slip trace at the maximum shear stress of notch. The phase of crack progress looks similar with Photo. 1(a), but around the crack, more pits and micro-cracks appeared. Especially, deducible area as dezincification phases formed broadly around the cracks and crack trace. Photo. 2(b) is a magnified picture of crack face of A in the Photo. 2(a). It shows that the pits and micro-cracks get connected as they formed more than Photo. 1(a). And also deducible area as dezincification phases found more.

3.3 Dezincification phases of crack area

For the quantitative study, the chemical compositions

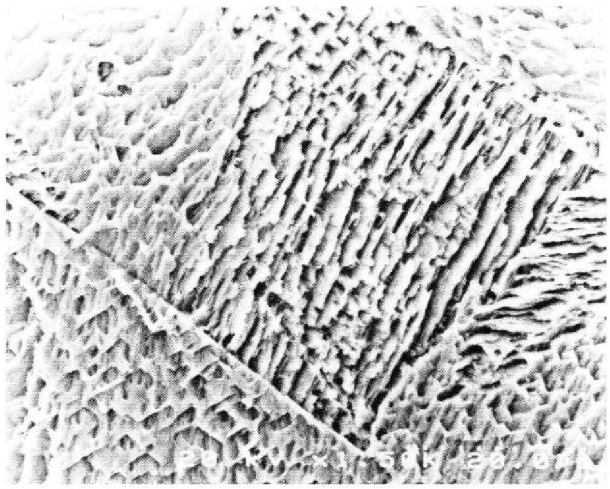

Photo. 3. SEM micrograph at the region of zincification

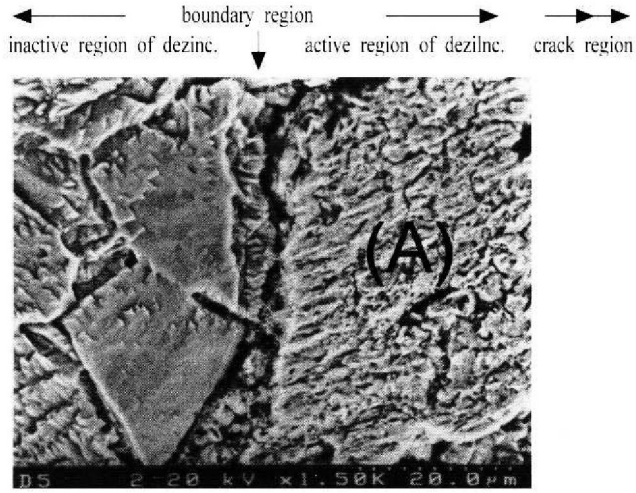

Photo. 4. SEM micrograph observed in 30℃, 3.5% NaCl + 0.1% NH_4OH solution(v = 5 m/s) at 75%σy(94 after test time 160(hr)

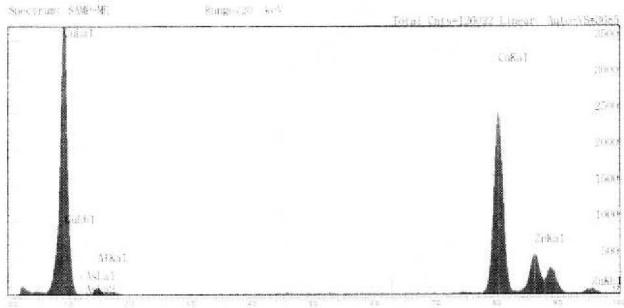

Chemical composition(Wt%)	Cu	Zn	Al	Fe	As	Pb
	76.0	22.03	1.85	0.05	0.02	0.05

Fig. 5. EDS spectrum of Al-brass material at the region of zincification

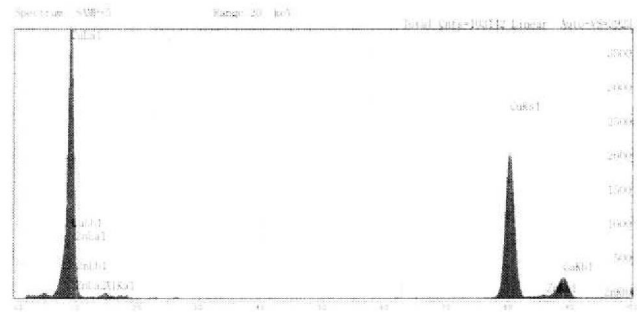

Chemical composition(wt%)	Cu	Zn	Al
	95.79	3.85	0.36

Fig. 6. EDS spectrum of (A) dezincification region in 30℃, 3.5% NaCl + 0.1% NH_4OH solutoin(v = 5 m/s) at 75%σy(94 MPa) after test time 160(hr)

analysis results of the dezincification boundary area using SEM and EDS showed in Photo. 3, Fig. 4, Photo. 4, Fig. , Photo. 5 and Fig. 6. Dezincification area were found at the surrounds of cracks in Photo. 1 and Photo. 2.

Photo. 3 is the picture of specimen taken by SEM which has no dezincification after stress corrosion cracking experiment. It is a structure of α/β-brass.[8] It shows that there are many lamellar twin phases which formed boundaries of polyhedrons orderly.

Fig. 5 shows the chemical compositions of the specimen analyzed using EDS. There is no dezincification after stress corrosion crack experiment. Zn part, compared with Table 1, shows the same amount, indicates that there are no dezincfication involved.

Photo. 4 is dezincification boundary taken by SEM around stress corrosion cracking in 30 ℃ solution. Those dezincification area almost consisted with pure α-brass.[9] It shows that there are lots of pits and micro-cracks caused by dezincification. And the dezincification influence area, left area of dezincifiction boundary, it shows that almost lamellar twin phase disappeared which was found in Photo. 3.

Fig. 6 shows chemical compositions analysis results of dezincifiction area appeared in Photo. 4 using EDS. It shows that Zn content reduced drastically compared with Fig. 5 where there is no dezincification.

Photo. 5 is dezincifiction boundary in 45 ℃ solution. It shows that there are more pits and cracks formed than Photo. 4. And the dezincification influence area, left area of dezincifiction boundary, it shows that almost lamellar twin phase disappeared.

Fig. 7 is chemical compositions analysis results of

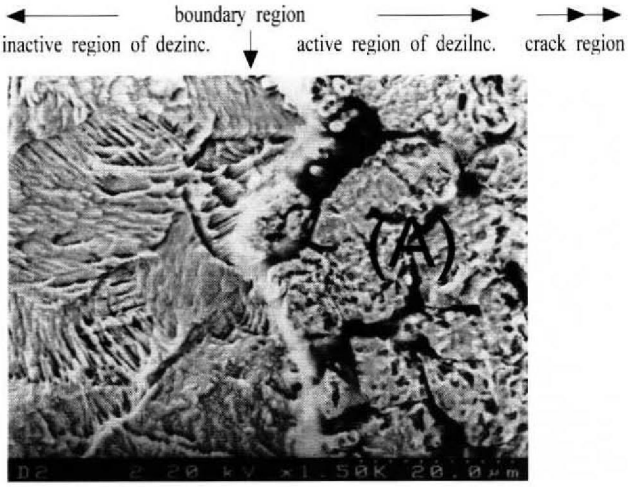

Photo. 5. SEM micrograph observed in 45℃, 3.5% NaCl + 0.1% NH_4OH solution(v = 5 m/s) at 75%σy(94 MPa)after test time 160(hr)

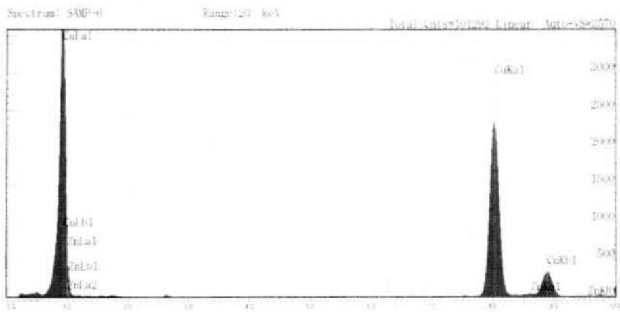

Chemical composition(wt%)	Cu	Zn	Al
	96.53	3.12	0.35

Fig. 7. EDS spectrum of (A) dezincification region in 45℃, 3.5% NaCl + 0.1% NH_4OH solutoin(v = 5 m/s) at 75%σy(94 MPa) after test time 160(hr)

dezincifiction area appeared in Photo. 5 using EDS. It shows that Zn content reduced drastically compared with Fig. 5 where there is no dezincification.

As studied in Photo. 3, Fig. 5, Photo. 4, Fig. 6, Photo. 5 and Fig. 7, actually Zn composition rate falls under 4% at the dezincification area of the crack trace. The reason for this is that Zn is detached prior to other compositions shown in Table 1 by localized preferential anodic dissolution(LPAD) effect.[10]

4. Conclusion

The test results on the effect of solution temperature on stress corrosion cracking of Al-brass in 3.5% NaCl + 0.1% NH_4OH solution under flow are as follows:

1) The latent time of stress corrosion cracking occurrence gets shorter, as the temperature gets higher.

2) Dezincification phase showed around the crack occupy wider range, as the temperature gets higher.

3) The pits as like micro-crack occurs at the periphery of stress corrosion cracking by dezincification and Zn composition falls under 4% at the dezincifiction area.

4) It is concluded that dezincification occurred by localized preferential anodic dissolution with stress focusing on stress corrosion cracking.

References

1. W. F. Brown Jr. and J. E. Srawley, "Plan Strain Crack Toughness Testing of High Strength Metallic Materials," ASTM STP 410
2. A. R. Jack and A. T. Price, "The initiation of fatigue cracks from notches in mild steel plates" *Int. J. offracture Mech.*, **6**(4), 401, (1970).
3. ASTM Standards, E407-99, Standard Practice for Microetching Metal and Alloys.
4. Hebrt H. Uhlig, Corrosion and Corrosion Control, p.326, (1991).
5. N. W. Polan, Metal Handbook, Vol. 13, Corrosion, 9th ed. ASM International, Metals Park, OH, p.614, (1987).
6. R. B. Mears, Symp. on Stress-Corrosion Cracking of Metals, ASTM-AIMME p.323, (1945).
7. A. V. Bobylev, Stress-Corrosion Cracking of Metals, Israel Program for Scientific Translation Ltd. (1961).
8. H. Schumann, Metallographie p.481, (1996).
9. H. Schumann, Metallographie p.488, (1996).
10. R. H. Heidersbach and E. D. Verink, *Corrosion*, **28**, 397, (1972).